Heterologous Avian System for Quantitative Analysis of Syncytin-1 Interaction with ASCT2 Receptor

Krystof Stafl
Institute of Molecular Genetics Czech Academy of Sciences: Ustav molekularni genetiky Akademie Ved Ceske Republiky

Martin Travnicek
Institute of Molecular Genetics Czech Academy of Sciences: Ustav molekularni genetiky Akademie Ved Ceske Republiky

Dana Kucerova
Institute of Molecular Genetics Czech Academy of Sciences: Ustav molekularni genetiky Akademie Ved Ceske Republiky

Lubomira Pecnova
Institute of Molecular Genetics Czech Academy of Sciences: Ustav molekularni genetiky Akademie Ved Ceske Republiky

Veronika Krchlikova
Institute of Molecular Genetics Czech Academy of Sciences: Ustav molekularni genetiky Akademie Ved Ceske Republiky

Eliska Galikova
Institute of Molecular Genetics Czech Academy of Sciences: Ustav molekularni genetiky Akademie Ved Ceske Republiky

Jiri Hejnar
Institute of Molecular Genetics Czech Academy of Sciences: Ustav molekularni genetiky Akademie Ved Ceske Republiky

Katerina Trejbalova (katerina.trejbalova@img.cas.cz)
Institute of Molecular Genetics Czech Academy of Sciences: Ustav molekularni genetiky Akademie Ved Ceske Republiky https://orcid.org/0000-0002-9872-3041

Research Article

Keywords: retroviral receptor, envelope glycoprotein, envelope-receptor interaction, ASCT2 (SLC1A5), Syncytin-1, cell-cell fusion, NanoLuc luciferase

Posted Date: February 24th, 2021

DOI: https://doi.org/10.21203/rs.3.rs-227071/v1

Abstract

Background

Human Syncytin-1 is an envelope glycoprotein of retroviral origin. After interaction with ASCT2, its cellular receptor, Syncytin-1 triggers cell-cell fusion and formation of a multinuclear syncytiotrophoblast layer of the placenta. The ASCT2 receptor is a multi-spanning membrane protein containing a protruding extracellular part called region C, which has been suggested to be a retroviral docking site. Precise identification of the interaction site between ASCT2 and Syncytin-1 is challenging due to the complex structure of ASCT2 protein and the background of endogenous *ASCT2* gene in the mammalian genome. Chicken cells lack the endogenous background and, therefore, can be used to set up a system with surrogate expression of the ASCT2 receptor.

Results

We have established a retroviral heterologous chicken system for rapid and reliable assessment of ectopic human ASCT2 protein expression. Our dual-fluorescence system proved successful for large-scale screening of mutant ASCT2 proteins. Using this system, we demonstrated that progressive deletion of region C substantially decreased the amount of ASCT2 protein production. In addition, we implemented quantitative assays to determine the interaction of ASCT2 with Syncytin-1 at multiple levels, which included binding of the soluble form of Syncytin-1 to ASCT2 on the cell surface and a luciferase-based assay to evaluate cell-cell fusions that were triggered by Syncytin-1. Finally, we restored the function of Syncytin-1 in a replication-competent retrovirus and assessed the infection of chicken cells expressing human ASCT2 by chimeric Syncytin-1-enveloped virus. The results of the quantitative assays showed that deletion of the major part of region C did not abolish the interaction of ASCT2 with Syncytin-1.

Conclusions

We present here a heterologous chicken system for effective assessment of the expression of transmembrane ASCT2 protein and its interaction with Syncytin-1. The system profits from the absence of endogenous ASCT2 background, and implements the quantitative assays to determine the ASCT2-Syncytin-1 interaction at several levels. Using this system, we demonstrated that the protruding region C of ASCT2 was essential for protein expression but not for the interaction with Syncytin-1 glycoprotein.

Background

Syncytin-1 was identified as an essential gene implicated in human placenta morphogenesis and function (1, 2). Specifically, it triggers the cell-cell fusion of cytotrophoblast and formation of multinucleated syncytiotrophoblast. The intrinsic fusogenic function of Syncytin-1 relates to its viral origin. The human *syncytin*-1 gene represents the retroviral *envelope* (*env*) of endogenous ERVW-1 provirus that had been exapted for placentation. To prevent undesirable formation of multinucleated

syncytia in non-placental tissues, *syncytin*-1 expression is restricted to the placenta by several mechanisms which include epigenetic modifications of the 5‘ LTR regulatory region of ERVW-1, availability of specific transcription factors and effective splicing of env mRNA that occurs exclusively in trophoblast and, aberrantly, in germ cell tumours (3–9). Once synthesised, the Syncytin-1 protein undergoes post-translational modifications, homo-trimer assembly, and cleavage of its surface (SU) and transmembrane (TM) subunits by cellular furin protease. Finally, Syncytin-1 is transported to the plasma membrane to exert its fusogenic function (10). Through the receptor-binding domain (RBD), the SU subunit of Syncytin-1 is responsible for binding to the specific cellular receptor (11). This interaction leads to Syncytin-1 conformational rearrangements that drive the membrane fusion process and multinucleated syncytium formation.

Two sodium-dependent neutral amino acid transporters, ASCT2 (SLC1A5) and, alternatively, ASCT1 (SLC1A4), were identified as Syncytin-1 cellular receptors (1, 12). Both proteins are widely expressed, including human placenta. Besides its role in trophoblasts fusion, ASCT2 as a cellular glutamine transporter was found to be overexpressed in various human tumours and is related to poor prognosis (13–15). The ASCT2 gene is present in most vertebrates, but importantly, it is missing in the chicken genome (16). ASCT2 serves as receptor for the entire RD114-and-D-type-retrovirus (RDR) interference group, which is comprised of distinct retroviruses isolated from different mammalian and avian hosts (17–19). Furthermore, the RDR-related envs exploiting ASCT2 as a specific receptor were identified in the genomes of several mammalian endogenous retroviruses (20–22). ASCT2 is organised as a homo-trimeric multi-membrane spanning protein with each monomer consisting of five extracellular loops (ECLs). ECL2 of ASCT2 folds into two extracellular parts that are separated by a short in-membrane region (Fig. 1c). The C-terminal part of ECL2, designated as region C, has been suggested to be critical for the interaction with Syncytin-1 (23). Cryo-electron microscopy of ASCT2 showed that region C protrudes from the cell surface into the extracellular space, and hence has been proposed as a retroviral docking site (24, 25). Furthermore, N-glycosylation at two sites within ECL2 has been shown to change the receptor affinity to envelope glycoproteins as well as receptor transport to the plasma membrane (12, 23, 26). Nevertheless, despite intensive study, the specific ASCT2 amino acid residues involved in the interaction with Syncytin-1 have not been identified.

Our understanding of the Syncytin-1-receptor interaction is complicated by the availability of two alternative receptors (ASCT1 and ASCT2) in mammalian cells and difficulties with manipulating integral transmembrane proteins. To define the molecular determinants of Syncytin-1 and its cellular receptor interaction, advanced systems that precisely monitor the receptor are highly required.

In this study, we present such a methodological approach by focusing on ASCT2 with a characterised structure as a proof of concept. We developed a novel dual-fluorescence system, FuTraP (Fusion Transmembrane Protein), for ectopic expression of human ASCT2 in chicken cells. To determine the ASCT2-Syncytin-1 interaction, we implemented several quantitative assays that allowed us to evaluate the binding of the soluble form of Syncytin-1 to ASCT2 and assess cell infection with a replication-competent reporter retrovirus with the Syncytin-1 envelope. Additionally, we developed a new quantitative

assay of cell-cell fusion based on a complementation of two-component luciferase. We have demonstrated that our chicken heterologous FuTraP system represents an efficient tool to study the interaction of Syncytin-1 and ASCT2 receptor.

Results

Avian retroviral vector pFuTraP expressing ASCT2

For ectopic expression of wild-type and mutated ASCT2, we chose to use the chicken cell system, which provided several advantages. i. The absence of the ASCT2 gene in the chicken genome (16) eliminates any background of endogenous ASCT2 gene product and its interference with the ectopically expressed protein. ii. Efficient ectopic expression of ASCT2 can be driven by a versatile avian replication-defective retroviral vector, which stably integrates in the chicken cell genome. iii. The interaction of Syncytin-1 with ASCT2 can be simulated by entry of a chimeric avian leukosis-based virus (ALV) carrying the Syncytin-1 envelope. iv. ASCT2-expressing and Syncytin-1-enveloped retroviral vectors can be easily produced in previously prepared chicken packaging cells and in the DF-1 chicken cell line, respectively.

We constructed a dual-fluorescence ASCT2 expression vector, designated here as pFuTraP-hA2, that contains wild-type human ASCT2 fused to the Green Fluorescent Protein from *Aequorea coerulescens* (AcGFP), followed by an IRES-iRFP713 cassette (Fig. 1a). We then transduced chicken DF-1 cells with VSV-G-pseudotyped viral particles carrying the FuTraP-hA2 genome and obtained cells expressing two proteins of the FuTraP system, specifically the ASCT2-AcGFP fusion protein, and iRFP713 protein. ASCT2-AcGFP permits exact quantification of the ASCT2 protein, which can be directly localised in the cell. iRFP713 translation occurs from the same mRNA as the ASCT2-AcGFP fusion protein but is initiated at the Internal Ribosome Entry Site (IRES) sequence. The fluorescence intensity of iRFP713 thus reflects the mRNA level of the FuTraP transcript and allows us to enrich the successfully modified cells regardless of the ASCT2 expression levels. After the transduction of DF-1 cells with the wild-type FuTraP-hA2 we sorted the cell population with efficient expression of the iRFP713 fluorescent protein (see the FuTraP-hA2 dot-plot in Fig. 1d in comparison to non-modified DF-1 cells used as negative control).

Next, to explore the role of region C that has been suggested as a retroviral docking site, we designed pFuTraP-d5 to pFuTraP-d22 mutants containing progressively extended deletions of five to 22 amino acids from the ASCT2 receptor region C (Fig. 1b). The largest deletion removed the entire region C. We also constructed a pFuTraP-N212Q mutant with abolished glycosylation within region C (Fig. 1b). Similarly to the wild-type FuTraP-hA2, we transduced DF-1 cells with the individual FuTraP mutants. After cell sorting, we obtained a similar fraction of iRFP713-positive cells for all transduced FuTraP variants, showing a comparable efficiency of our technique (Fig. 1d). The mean fluorescence intensity (MFI) of iRFP713 was about two times higher in the deletion mutants in comparison to wild-type ASCT2 (Fig. 1d,e), reflecting differences in the mRNA production or stability.

The ASCT2 protein level affected by deletion of region C

The fluorescence intensity of AcGFP, which was C-terminally fused to the wild-type or mutant receptor, monitored expression of the ASCT2 protein. Since it was difficult to separate the AcGFP-positive and AcGFP-negative populations in some of the mutants (Fig. 1d), we evaluated the MFI of AcGFP for the entire cellular population (Fig. 1f). MFI of the non-modified DF-1 cell line served as the negative control. We observed that deletion of seven or more amino acids of region C led to a substantial decline of the ASCT2 protein amount when compared to the wild-type ASCT2 (Fig. 1f). The protein level of the FuTraP-d22 mutant showed no difference compared to the DF-1 negative control. The ratio of AcGFP intensity that reflected the level of the protein (Fig. 1f) to the iRFP713 intensity that reflected the mRNA level (Fig. 1e) indicated that progressive deletions of five or more amino acids of region C decreased the protein production/stability (Fig. 1g). On the other hand, according to AcGFP to iRFP713 ratio, the protein amount of FuTraP-N212Q glycosylation mutant was comparable to the wild-type, at least in the avian system (Fig. 1g). Our results revealed that region C was essential for the protein expression/stability of ASCT2.

ASCT2 cell surface localisation and receptor function

The correct display of the ASCT2 protein on the cell surface is crucial for its receptor function. To track ASCT2 localisation, we used confocal microscopy on a selected panel of ASCT2 mutants. Wild-type human ASCT2 localised preferentially to the cell surface, which was visualised after fluorescent staining of cellular membrane (Fig. 2, blue channel, middle right). Similarly, both the FuTraP-d5 deletion mutant and the FuTraP-N212Q glycosylation mutant preferentially localised to the cell surface (Fig. 2). Corresponding to the FACS results, the FuTraP-d11, FuTraP-d15, and FuTraP-d22 mutants displayed a sharp reduction in the ASCT2 protein amount, while their cellular localisation could not be determined (Fig. 2). In contrast to AcGFP, iRFP713 was distributed throughout the entire cell, including the nucleus, in all FuTraP variants (Fig. 2, red channel, left).

To further examine the ASCT2 display and its binding to Syncytin-1, we adapted immunoadhesin, a soluble fusion protein that combines the target-binding region of a ligand with the Fc region of an IgG (27–29). We prepared the soluble form of Syncytin-1 (sS1) consisting of Syncytin-1 RBD fused with the heavy chain of rabbit IgG (Fig. 3a). Selected panel of cells expressing ASCT2 variants were incubated with sS1 and the binding to the ASCT2 receptor on the cell surface was visualised by means of an Alexa Fluor 594-conjugated anti-IgG antibody. Non-modified DF-1 cells labelled with sS1 served as a negative control. Flow cytometry analysis showed a specific shift in Alexa Fluor 594 staining, demonstrating the binding of sS1 to the wild-type FuTraP-hA2 (Fig. 3b). The FuTraP-d5 deletion mutant and the FuTrap-N212Q glycosylation mutant bound sS1 even better than the wild-type. The FuTraP-d7 binding of sS1 was similar to the wild-type. The results further showed that FuTraP-d11, FuTraP-d15, and FuTraP-d22 deletions of region C led to a decreased interaction of ASCT2 mutants with the sS1, which was similar to the negative control (Fig. 3b). The results confirmed the surface localisation of the ASCT2 receptor expressed from the pFuTraP vector, hence demonstrated the functional interaction of the receptor with the soluble form of Syncytin-1. These observations further supported the decreased surface display of ASCT2 mutants missing 11 or more amino acids of region C.

ASCT2 receptor mediates entry of Syncytin-1-enveloped virus

To explore the ASCT2 capacity to mediate retroviral cellular entry, we adapted the human Syncytin-1 glycoprotein to act as a functional envelope protein of infectious avian retrovirus. We constructed the chimeric replication-competent pMCAS(Sync1-MSC16)dsRed vector, in which Syncytin-1 glycoprotein replaced the original envelope of ALV. After elimination of a cryptic splicing acceptor site and shortening the cytoplasmic domain of Syncytin-1 to 16 amino acids (10) (Fig. 4a), we obtained the infectious MCAS(Sync1-MSC16)dsRed virus produced in the supernatant of transfected DF-1 cells. The virus reached a titre of 10^4 IU/mL and was used to infect the cells with the multiplicity of infection 0.1 to 0.4. The Syncytin-1-enveloped virus specifically entered cells expressing the wild-type FuTraP-hA2 as we identified by dsRed fluorescence detected microscopically or by flow cytometry (14% dsRed-positive cells, Additional File 1: Fig. S1). Based on the virus titre and percentage of dsRed-positive cells, we calculated the cellular sensitivity to viral infection, which corrects for the possible simultaneous co-infections of the same cell (Fig. 4b). Importantly, no viral infection of non-modified DF-1 chicken cells was detected (Fig. 4b, Additional File 1: Fig. S1). It is of note that the infectivity of the replication-competent retrovirus with Syncytin-1 envelope validates the supposed original function of Syncytin-1 as an envelope of ancestral exogenous retrovirus.

To determine whether deletion mutants can serve as a receptor for the Syncytin-1-enveloped virus, we infected DF-1 cells carrying ASCT2 variants with the MCAS(Sync1-MSC16)dsRed virus. Both deletion mutants FuTraP-d5 and FuTraP-d7 and glycosylation mutant FuTraP-N212Q conferred higher sensitivity to infection in comparison to the ASCT2 wild-type FuTraP-hA2 (Fig. 4b). On the other hand, cells carrying FuTraP-d11 and larger deletions displayed reduced sensitivity to infection compared to cells carrying the wild-type FuTraP-hA2 (Fig. 4b). However, all deletion mutants, including those with a deletion of the entire region C, displayed some level of susceptibility to infection when compared to non-modified DF-1 chicken cells (Fig. 4b).

Because the sensitivity of cells modified with ASCT2 variant may depend on the amount of the receptor, we normalised the cellular sensitivity to infection (calculated from the fraction of dsRed-positive cells, Fig. 4b) to the receptor protein level (AcGFP MFI of non-infected cells measured in the same experiment). The normalised FuTraP-d5 receptor sensitivity was slightly, although significantly lower than the wild-type (Fig. 4c). Interestingly, deletion of seven to 17 amino acids of region C increased the normalised receptor sensitivity to Syncytin-1 in comparison to the wild-type (Fig. 4c). Deletion mutants FuTraP-d19 and FuTraP-d22 normalised to the ASCT2 protein level were still significantly more susceptible to the Syncytin-1-enveloped virus than the non-modified DF-1 cells (Fig. 4c). After normalisation to the ASCT2 protein level, the glycosylation mutant revealed a similar sensitivity to Syncytin-1 as observed in the wild-type (Fig. 4c). These results demonstrate that the deletion of the putative retrovirus docking site did not abolish the ASCT2 receptor interaction with the Syncytin-1 envelope.

Cell-cell fusion triggered by Syncytin-1

Finally, we focused on the cell-cell fusion triggered by the ASCT2-Syncytin-1 interaction. We constructed the non-infectious retroviral pMCAS(3Flag-Sync1-MS)dsRed expression vector. In this construct, the original ALV retroviral envelope was replaced by the Syncytin-1 glycoprotein, which was fused N-terminally to the three-Flag epitope, had mutated the cryptic splicing acceptor site and contained the entire open reading frame (Fig. 5a). After transfection of ASCT2-expressing cells with the pMCAS(3Flag-Sync1-MS)dsRed no infectious viral particles were produced, but importantly, we observed cell-cell fusion that further supported the correct ASCT2 surface localisation and receptor function (Additional File 2: Fig. S2, Additonal File 4: Movie).

To quantify cell-cell fusion, we utilised the NanoLuc Binary Technology (NanoBiT), where the High-Affinity NanoBiT (HiBiT) subunit spontaneously complements the Large NanoBiT (LgBiT) subunit to form a functional NanoLuc luciferase enzyme (Fig. 5b).

We engineered DF-1 cells that stably expressed either LgBiT or HiBiT and modified them to express ASCT2 variants or fusogenic Syncytin-1, respectively. FuTraP-hA2 and FuTraP-d5, FuTraP-d11, FuTraP-d15, FuTraP-d22 were transduced into DF-1/LgBiT cells and the iRFP713-positive populations were separated by cell sorting. The pMCAS(3Flag-Sync1-MS)dsRed vector was transfected into DF-1/HiBiT cells, and a transfection efficiency of 45% was determined according to dsRed fluorescence (Additional File 3: Fig. S3). Anti-Flag cell labelling showed that 40% of the transfected cells expressed Syncytin-1 on the cell surface (Additional File 3: Fig. S3).

Finally, DF-1/LgBiT cells expressing FuTraP variants were seeded together with DF-1/HiBiT cells that had been transfected with Syncytin-1, and cell-cell fusion was quantified as NanoLuc luciferase luminescence (Fig. 5c). DF-1/LgBiT cells without ASCT2 mixed with DF-1/HiBiT-Syncytin-1 cells were used as a negative control. Our results revealed a similar intensity of cell-cell fusion triggered by the wild-type FuTraP-hA2 and FuTraP-d5 mutants (Fig. 5c). In contrast, increasing the extent of deletion within region C led to a decrease in the fusion ability of FuTraP-d11, FuTraP-d15, and FuTraP-d22 mutants. Nevertheless, the fusion activity of the mutants was higher than that of the negative control (Fig. 5c). Our results further confirmed that the interaction of Syncytin-1 with the ASCT2 expressed from the dual-reporter FuTraP system triggered cell-cell fusion. The luciferase fusion assay corroborated our conclusions that progressive deletions of region C reduced ASCT2 cell surface expression but did not disrupt its interaction with the Syncytin-1 envelope glycoprotein.

Discussion

We have elaborated a heterologous retroviral system, FuTraP, for precise analysis of the ASCT2 protein amount and cell membrane localisation. Our system allows quantitative assessment of the ASCT2-Syncytin-1 interaction at multiple levels including Syncytin-1 binding, membrane fusion, and cellular entry of the Syncytin-1-enveloped virus. Our report demonstrates another advantage of the presented system, which consists of accessible large-scale screening of ASCT2 mutants. The presented system can be easily modified for analyses of the interactions between different RDR Envs and ASCT2 or ASCT1

receptors. Additionally, we propose that the FuTraP system would be suitable for expression of other transmembrane proteins and analysis of their receptor interactions.

We suggest that the FuTraP system will be useful for further studies of ASCT2 interaction. The precise site of interaction with Syncytin-1 has not been yet identified, despite extensive analyses performed using human, mouse, and hamster ASCT2 chimaeras and glycosylation mutants (1, 12). The findings of previous studies pointed to the role of region C (23), which can be interpreted either as the viral attachment site or the negative control region inhibiting access of Syncytin-1 to an unidentified interaction site. We tried to resolve the question but our initial experiments were limited by inefficient expression and mislocalisation of ASCT2 variants bearing deletions of region C. This led us to development of the FuTraP system.

The FuTraP system allows multi-level assessment in single cytometry measurement. The dual-fluorescence arrangement enables us to easily distinguish between whether reduced Syncytin-1-receptor interaction is due to mutation of the interaction site or decreased ASCT2 protein amount. This system has proved to be essential in the analysis of ASCT2 region C deletion mutants. The measurement of iRFP713 fluorescence validated a similar mRNA amount for all deletion variants, while AcGFP fluorescence clearly demonstrated that progressive deletion of the protruding region C substantially decreased the amount of ASCT2 protein within the cells.

To explore the interaction of ASCT2 variants with Syncytin-1, we adapted an immuoadhesin assay that detected binding of the sS1 to the ASCT2 receptor. The assay reflected the attachment of Syncytin-1 RBD to the receptor regardless of the following steps of virus entry. This technique further proved the surface localisation of ectopically expressed ASCT2 and specificity of binding to Syncytin-1. Nevertheless, as it was based on labelling of individual receptor molecules, the method was less sensitive than the tests of virus infectivity or the fusion assay and was substantially dependent on the level of receptor expression on the cell surface. The results are in accordance with the other measurements and imply that the distal part of region C is not responsible for the interaction with Syncytin-1.

Next, we modified Syncytin-1 to function as the envelope of chimeric infectious avian retrovirus. Although Syncytin-1 has been shown to pseudotype lentiviral particles (12, 23), our results demonstrate successful recovery of the endogenous Syncytin-1 glycoprotein as an envelope of a replication-competent retrovirus. We have shown that in addition to promoting cell-cell fusion, Syncytin-1 can perform its expected original function, i.e., mediate infection of cells that express the specific receptor.

Based on the cellular sensitivity, we suggest that ASCT2 was susceptible to Syncytin-1 infection after deletion of 17, and even 19 and 22, amino acids from region C. We detected a sharp decline in receptor sensitivity when comparing FuTraP-d17 and FuTraP-d19 mutants (Fig. 4b,c). Surprisingly, FuTraP-d22 was still sensitive to infection although we have not detected production of mutant protein by means of AcGFP MFI (Fig. 1f). However, we have assumed that a very low level of FuTraP-d22 protein was still produced (see the corresponding dot-plot on Fig. 1d), and was sufficient to confer susceptibility towards Syncytin-1. This observation approves that the cellular entry of the Syncytin-1-enveloped virus would be

the most sensitive assay to disclose functional Syncytin-1-receptor interaction, especially under the conditions of reduced protein level of receptor variants. In summary, the results of the virus infection assay indicate that region C, at least its distal 17 amino acids, does not represent the interaction site with Syncytin-1 glycoprotein.

Our system further supported normalisation of the receptor sensitivity, which we calculated as the ratio of cells sensitive to infection to the amount of ASCT2 protein (Fig. 4c). This normalisation revealed that the FuTraP-d7 deletion mutant displayed a higher receptor sensitivity than the wild-type and FuTraP-d5 deletion mutant. This result could indicate the inhibitory effect of a most distal part of human region C on the interaction with Syncytin-1. However, this hypothesis requires further investigation.

The ECL2 region of ASCT2 contains two glycosylated asparagine residues - N163 and N212. Creation of a double mutant in which both glycosylations were eliminated was shown to alter the ASCT2 protein level and localisation (26). We mutated the N212 glycosylation site within region C and assessed the single glycosylation mutant for sensitivity to Syncytin-1 infection. Importantly, we confirmed that the FuTraP-N212Q mutant was correctly expressed and localised on the surface of avian DF-1 cells. Our results did not show any effect of N212 glycosylation on the interaction with Syncytin-1.

Importantly, our experiments demonstrated that non-modified DF-1 cells were not sensitive to Syncytin-1-enveloped virus at all, underlining the benefits of the heterologous chicken system. The zero background means that chicken ASCT1 is not compatible with Syncytin-1. Thus, the surrogate human ASCT1 or ASCT2 expression in our system can help in understanding of the individual contribution of ASCT1 and ASCT2 to the fusogenic capacity of human trophoblast. It is not clear whether both alternative receptors have equal and additive effects or whether one of them is the major player in the cell-cell fusion process.

Finally, we explored the intensity of cell-cell fusion induced after Syncytin-1 interaction with the ASCT2 variants. Cell-cell fusion is routinely detected by May-Grünwald and Giemsa staining followed by microscopic techniques, optionally using indicator cells expressing β-galactosidase or GFP (1, 2, 12, 23, 30, 31). In this case, quantitation is achieved by nuclei and syncytia counting and/or by colorimetric assays. Recently, complementation of a reporter protein, either GFP or luciferase, was introduced to quantify cell-cell fusion (32–34). To quantitatively assess Syncytin-1-triggered cell-cell fusion, we adapted the NanoLuc Binary Technology complementation assay. We selected this technology because it uses NanoLuc luciferase, which produces high intensity, glow-type luminescence after spontaneous assembly of High-Affinity NanoBiT and Large NanoBiT subunits. These parameters provided high-sensitivity quantitative measurement of the cell-cell fusion. The assay confirmed differences in the fusion ability among the ASCT2 mutants. Similarly to the assessment of virus infection, we detected a functional interaction between Syncytin-1 and all ASCT2 variants. Our results propose the solution of “region C puzzle” and favour the interpretation of region C inhibiting the access of Syncytin-1 to the binding site on the receptor (23). These results imply that while region C is essential for the receptor surface expression, it is not responsible for the interaction with Syncytin-1.

Conclusions

We introduce FuTraP, a novel system to study expression and interaction of transmembrane proteins based on fluorescent and luminescent techniques. We employed FuTraP for heterologous ectopic expression of the human ASCT2 receptor in chicken cells. We have demonstrated the benefits of FuTraP on a panel of ASCT2 mutants containing deletions within the region C of extracellular loop 2. We have shown that the deletion of a major part of region C affected ASCT2 protein level. Region C was earlier proposed as the part of the receptor that is crucial for the docking of several retroviruses. We focused on the interaction of ASCT2 with Syncytin-1, an envelope of human endogenous retrovirus. To evaluate the interaction of ASCT2 mutants with Syncytin-1, we developed sensitive assays that measured soluble Syncytin-1 binding, sensitivity to infectious virus and cell-cell fusion. We have demonstrated that glycosylation of region C is not required for the interaction of Syncytin-1 and ASCT2. Further, our results show that the deletions of region C do not abolish the receptor function. Our system can facilitate precise characterisation of the Syncytin-1 binding site on the receptor and lead to the detailed molecular understanding of one of the critical steps in human placenta morphogenesis.

Methods

Cloning of expression vectors and viruses

Sequences of all constructs used in the study are accessible in Additional Files 5 to 17. Coding sequences of human ASCT2 and Syncytin-1 were amplified from the BeWo choriocarcinoma cell line cDNA. cDNA was synthesised by AccuScript polymerase (Agilent) with oligo(dT) primers. The sequences corresponded to GenBank NP_005619.1 and NP_001124397.1, respectively. For all cloning steps, an In-Fusion Cloning Kit (TaKaRa) was used.

The pFuTraP vector (Fig. 1a) was based on replication-deficient avian retroviral vector pRNIG used in our laboratory (35). pFuTraP contained LTR sequences derived from Myeloblastosis Associated Virus (MAV, GenBank accession No. L10922.1, (36)) and the encapsidation signal from RCASBP (37). Downstream of the encapsidation signal, a Kozak's sequence, and the human ASCT2 coding sequence were cloned. Human ASCT2 possessed a mutated stop-codon, which allowed a read-through into GGGGS linker, and AcGFP fused in-frame. The IRES sequence derived from the encephalomyocarditis virus was placed downstream of ASCT2, which ensured translation of iRFP713, the far-red fluorescence protein. The vector was propagated in the Stbl2 strain of *E. coli*. pFuTraP containing the wild-type human ASCT2 was designated pFuTraP-hA2. pFuTraP containing deletions of 5 to 22 amino acids within region C were designated pFuTraP-d5 to pFuTraP-d22. Within the deletion mutants, we inserted two glycines instead of the deleted amino acids to compensate for the loop flexibility. We cloned the following deletion mutants: pFuTraP-d5, pFuTrap-d7, pFuTraP-d11, pFuTraP-d13, pFuTraP-d15, pFuTraP-d17, pFuTraP-d19, pFuTraP-d22 (Fig. 1b). pFuTraP containing the ASCT2 N212Q glycosylation mutant was designated pFuTraP-N212Q (Fig. 1b).

pMCAS(Sync1-MSC16)dsRed (Fig. 4a) was a replication-competent avian retrovirus based on high titer RCASBP (37, 38). The LTR sequences were derived from MAV, the syncytin-1 coding sequence replaced the original ALV *env* gene, and the dsRed coding sequence was cloned downstream of the splice acceptor instead of the original v-*src* gene. The signal peptide of the *Syncytin-1* gene was replaced with the signal peptide of the ALV *env*(*A*) gene. The cryptic splice acceptor identified within the syncytin-1 coding sequence (39) was mutated to increase the ratio of spliced syncytin-1 mRNA to spliced dsRed mRNA. To obtain infectious Syncytin-enveloped virions, a stop codon was introduced after 16 amino acids of the cytoplasmic tail as previously described (10) (Fig.4a). After transfection of pMCAS(Sync1-MSC16)dsRed, infectious viral particles were produced; however, after the first round of infection, the virus was not spreading further. In contrast, pMCAS(3Flag-Sync1-MS)dsRed (Fig. 5a) expressing Syncytin-1 with the unshortened cytoplasmic tail did not produce infectious viral particles. In this vector, Syncytin-1 was fused N-terminally with the three-Flag epitope (Fig. 5a). Both vectors were manipulated at the BSL2 containment level.

Cell lines, transfections, transductions, and infections

Both chicken fibroblast cell line DF-1 (40) and Avipack packaging cell line (41) used in experiments were cultured in DMEM:F12 media (Sigma), supplemented with 4% fetal bovine serum, 4% bovine serum, and 1% chicken serum in 5% CO_2 atmosphere at 37 °C. One hundred µg of penicillin and 100 µg streptomycin per millilitre of media were added. For all transfections, Lipofectamine 3000 (Thermofisher) was used according to the manufacturer's instructions on cells in the exponential phase of growth.

To achieve stable ectopic expression of human ASCT2 variants, the FuTraP genome was transduced into target DF-1 cells by infection with VSV-G-pseudotyped viral particles. Transducing viruses were produced in the Avipack cell line after co-transfection of a 35-mm dish with 0.5 µg pVSV-G (Clontech), 0.75 µg pcgag-pol (35), and 1.25 µg pFuTraP. The supernatant containing the transducing virus was collected three days after transfection, filtered through a 0.45 µm filter, and applied to a 35-mm dish with 0.15×10^6 DF-1 cells. Modified cells were cultivated for one week followed by sorting of the iRFP713-positive cell population. The sorted cells were expanded for another week and sorting of the iRFP713-positive population was repeated.

Infectious virus MCAS(Sync1-MSC16)dsRed was produced by transfection of DF-1 cells; the supernatant was collected and filtered 2 – 3 days after the transfection. Infections were performed as follows: 0.1×10^6 of DF-1 cells expressing the variants of pFuTraP were seeded one day before infection on 12-well plate; cells were infected with 1 mL of virus supernatant; the supernatant was replaced with fresh media one day post-infection; three days post-infection the cells were fixed in 1-2% paraformaldehyde (final concentration), analysed by flow cytometry, and a fraction of infected cells was detected by dsRed fluorescence (Additional File 1: Fig. S1).

The sensitivity of cells was calculated using the following formula: $sensitivity = -\ln(1 - fraction\ of\ dsRed\text{-}positive\ cells)$ (42). The sensitivity was further normalised to the sensitivity of FuTraP-hA2.

Soluble Syncytin-1-immunoadhesin binding

Construction of the soluble form of Syncytin-1 pSU(S1)-RBD-IgG (Fig. 3a) was based on immunoadhesin previously used in ALV receptor studies (28, 29). pSU(S1)-RBD-IgG contained a signal peptide of ALV *env*(*A*) followed in-frame by Syncytin-1 amino acids 23 to 152 of the SU subunit containing the putative RBD (11). By means of a nine amino acid linker (Tobacco Etch Virus protease recognition sequence), the specified RBD of Syncytin-1 was fused to amino acids 175 to 402 of the constant region of the rabbit immunoglobulin G gene (GenBank Accession No. K00752.1). The resulting gene was inserted into the replication-competent avian retroviral vector pRCASBP(B) 3' to the ALV env(B) gene and downstream to the second splice acceptor site (Fig. 3a). After transfection of pSU(S1)-RBD-IgG into the DF-1 cells, the replication-competent virus with the ALV envelope (subgroup B) was spread throughout the permissive cell culture and, in addition, the infected cells produced the soluble form of Syncytin-1 (sS1) in the supernatant. After three passages of transfected cells, the supernatant was collected, filtered through 0.45 µm filter, aliquoted, and stored at −80 °C.

To measure the binding of the sS1, DF-1 cells modified with the FuTraP variants were detached using a non-enzymatic cell dissociation solution (Sigma) and 1×10^6 cells were incubated with 1 ml of supernatant containing the sS1 at 4 °C for 1 h. The cells were washed three times with PBS supplemented with 2% bovine serum. Then the cells were incubated for 30 min at 4 °C with anti-rabbit IgG conjugated to Alexa Fluor 594 antibody (1:1000 dilution in PBS with 2% bovine serum). After staining, the cells were washed three times in PBS supplemented with 2% bovine serum. Flow cytometry analysis was performed and the median fluorescence intensity of Alexa Fluor 594 was determined. Non-modified DF-1 cells were stained using the entire protocol as a negative control.

Microscopy

The cells were seeded on a microscope cover glass (0.15×10^6 cells per 35-mm dish with the cover glass) and incubated overnight. The next day, the cells were fixed in 4% paraformaldehyde, washed with PBS, stained with membrane dye CellBrite Blue (Biotium) according to the manufacturer's protocol, mounted in PBS, and visualised using confocal microscope Leica TCS SP8 with 63×/1.4 NA objective.

Images were deconvolved by Huygens software and contrast was enhanced using ImageJ.

NanoBiT Luciferase-based live-cell assay for cell-cell fusion quantification

To quantify cell-cell fusion, we adapted NanoBiT technology based on two-subunit NanoLuc luciferase (Nano-Glo® HiBiT system, Promega). We separately transfected linearized vectors containing two fragments of the luciferase enzyme – LgBiT and HiBiT (Promega) – into the DF-1 cells. Stable cell lines expressing either LgBiT or HiBiT proteins were obtained after two-week selection in the presence of Hygromycin B (0.2 mg/ml). The DF-1/LgBiT cells were transduced with FuTraP variants and subjected to two successive sortings for the iRFP713-positive population. The DF-1/HiBiT cells were then seeded in a 6-well plate (0.45×10^6 cells/well) and after 24 hrs transfected with 2.5 µg of pMCAS(3Flag-Sync1-

MS)dsRed. Forty-eight hrs after transfection, the DF-1/HiBiT-Sync1 cells were mixed with DF-1/LgBiT-pFuTraP cells in ratios 2×10^4 : 1×10^4 cells, respectively, and transferred in triplicate to a whole-white 96-well plate (Costar, flat bottom tissue culture treated, polystyrene). After 24 hr incubation, the supernatant from the cells was replaced with 100 µl of OptiMEM medium and the cells were incubated for additional 60 minutes. Afterwards, 20 µl of 37 °C-equilibrated Nano-Glo Live Cell Reagent (19 µl of LCS Dilution Buffer and 1 µl of Live Cell Substrate; Promega) containing the luciferase substrate, furimazine, was added to cells and the plate was placed on an orbital shaker at 300 rpm, 15 sec. At this point, reassorted HiBiT-LgBiT fragments in the fused cells started to oxidise the substrate, resulting in luminescence emission. The relative luminescence was measured in an EnVision Plate Reader (PerkinElmer) right after adding the Live Cell Reagent.

To verify the surface expression of 3Flag-Sync1-MS, living cells were immunostained 48 hrs after the transfection with monoclonal Anti-Flag® M2-FITC antibody (Sigma, 1:1000 dilution in PBS with 2% calf serum; 1 ml per 10^6 cells) and evaluated by flow cytometry. A live gate was created according to Hoechst 33258 staining. Transfection efficiency was assessed by flow cytometry according to the dsRed fluorescence (Additional File 3: Fig. S3).

Statistical analysis

For statistical analysis of the intergroup specificity, GraphPad Prism software (version 5.04) with a non-parametric two-tailed Mann-Whitney test was employed. Calculated P-values were depicted as follows: ** < 0.01, * < 0.05, ns > 0.05.

Abbreviations

AcGFP, *Aequorea coerulescens* Green Fluorescent Protein;

ALV, Avian Leukosis Virus;

ASCT, Alanine, Serine, Cysteine Transporter;

ECL, Extracellular Loop;

FITC, Fluorescein Isothiocyanate;

FuTraP, Fusion Transmembrane Protein;

HiBiT, High-Affinity NanoBiT;

IRES, Internal Ribosome Entry Site;

iRFP, Infrared Fluorescent Protein 713;

LgBiT, Large NanoBiT;

MAV, Myeloblastosis Associated Virus;

MFI, Mean Fluorescence Intensity;

NanoBiT, NanoLuc Binary Technology;

RBD, Receptor-Binding Domain;

RCASBP, Replication-Competent ALV LTR with Splice Acceptor and Bryan Polymerase;

RDR, RD114-and-D-type-retrovirus;

SLC, Solute Carrier;

SU, Surface subunit;

sS1, Soluble form of Syncytin-1;

TM, Transmembrane subunit;

Declarations

Ethics approval and consent to participate

Not applicable.

Consent for publication

Not applicable.

Availability of data and materials

The datasets supporting the conclusions of this article are included within the article and its additional files.

Competing interests

The authors declare that they have no competing interests.

Funding

This work was supported by the Czech Science Foundation (grant 17/14356S to JH), and by Preamium Academiae Grant awarded by the Czech Academy of Sciences to JH. The work was also supported by GA UK No. 554219 awarded by Charles University in Prague to KS.

Authors' contributions

KS conceived and designed the experiments, performed molecular cloning, cell and viral manipulations, flow cytometry analyses, infectivity assay, microscopy, analysed the data, and was a major contributor in writing the manuscript. MT conceived and designed the experiments, performed fusion assay, analysed the data. DK, LP and EG performed molecular cloning. VK performed confocal microscopy. JH conceived the research and was a major contributor in writing the manuscript. KT conceived the research and designed the experiments, performed molecular cloning, cell and viral manipulations, flow cytometry analyses, binding of sS1, analysed the data, and was a major contributor in writing the manuscript. All authors read and approved the final manuscript.

Acknowledgements

We acknowledge the Light Microscopy Core Facility, IMG CAS, Prague, Czech Republic, supported by MEYS (LM2018129, CZ.02.1.01/0.0/0.0/18_046/0016045) and RVO: 68378050-KAV-NPUI, namely Ivan Novotný and Helena Chmelová, for their support with the confocal and widefield imaging presented herein. We thank Zdeněk Cimburek and Matyáš Šíma from the Service Laboratory of Flow Cytometry, for their perfect technical assistance with the cell sorting and flow cytometry. We acknowledge Jasper Manning and Šárka Takáčová for language editing. We thank to Daniel Elleder, Ivan Hirsch, Filip Šenigl, and Karolína Pokorná for critical reading and comments.

References

1. Blond JL, Lavillette D, Cheynet V, Bouton O, Oriol G, Chapel-Fernandes S, et al. An envelope glycoprotein of the human endogenous retrovirus HERV-W is expressed in the human placenta and fuses cells expressing the type D mammalian retrovirus receptor. Journal of virology. 2000;74(7):3321-9.
2. Mi S, Lee X, Li X, Veldman GM, Finnerty H, Racie L, et al. Syncytin is a captive retroviral envelope protein involved in human placental morphogenesis. Nature. 2000;403(6771):785-9.
3. Gimenez J, Montgiraud C, Oriol G, Pichon JP, Ruel K, Tsatsaris V, et al. Comparative methylation of ERVWE1/syncytin-1 and other human endogenous retrovirus LTRs in placenta tissues. DNA research : an international journal for rapid publication of reports on genes and genomes. 2009;16(4):195-211.
4. Matouskova M, Blazkova J, Pajer P, Pavlicek A, Hejnar J. CpG methylation suppresses transcriptional activity of human syncytin-1 in non-placental tissues. Exp Cell Res. 2006;312(7):1011-20.
5. Trejbalova K, Blazkova J, Matouskova M, Kucerova D, Pecnova L, Vernerova Z, et al. Epigenetic regulation of transcription and splicing of syncytins, fusogenic glycoproteins of retroviral origin. Nucleic acids research. 2011;39(20):8728-39.
6. Benesova M, Trejbalova K, Kucerova D, Vernerova Z, Hron T, Szabo A, et al. Overexpression of TET dioxygenases in seminomas associates with low levels of DNA methylation and hydroxymethylation. Molecular carcinogenesis. 2017;56(8):1837-50.
7. Lin C, Lin M, Chen H. Biochemical characterization of the human placental transcription factor GCMa/1. Biochem Cell Biol. 2005;83(2):188-95.

8. Prudhomme S, Oriol G, Mallet F. A retroviral promoter and a cellular enhancer define a bipartite element which controls env ERVWE1 placental expression. Journal of virology. 2004;78(22):12157-68.
9. Benesova M, Trejbalova K, Kovarova D, Vernerova Z, Hron T, Kucerova D, et al. DNA hypomethylation and aberrant expression of the human endogenous retrovirus ERVWE1/syncytin-1 in seminomas. Retrovirology. 2017;14(1):20.
10. Cheynet V, Ruggieri A, Oriol G, Blond JL, Boson B, Vachot L, et al. Synthesis, assembly, and processing of the Env ERVWE1/syncytin human endogenous retroviral envelope. Journal of virology. 2005;79(9):5585-93.
11. Cheynet V, Oriol G, Mallet F. Identification of the hASCT2-binding domain of the Env ERVWE1/syncytin-1 fusogenic glycoprotein. Retrovirology. 2006;3:41.
12. Lavillette D, Marin M, Ruggieri A, Mallet F, Cosset FL, Kabat D. The envelope glycoprotein of human endogenous retrovirus type W uses a divergent family of amino acid transporters/cell surface receptors. Journal of virology. 2002;76(13):6442-52.
13. Guo H, Xu Y, Wang F, Shen Z, Tuo X, Qian H, et al. Clinical associations between ASCT2 and pmTOR in the pathogenesis and prognosis of epithelial ovarian cancer. Oncol Rep. 2018;40(6):3725-33.
14. Scalise M, Pochini L, Console L, Losso MA, Indiveri C. The Human SLC1A5 (ASCT2) Amino Acid Transporter: From Function to Structure and Role in Cell Biology. Front Cell Dev Biol. 2018;6:96.
15. Zhang Z, Liu R, Shuai Y, Huang Y, Jin R, Wang X, et al. ASCT2 (SLC1A5)-dependent glutamine uptake is involved in the progression of head and neck squamous cell carcinoma. British journal of cancer. 2020;122(1):82-93.
16. Gesemann M, Lesslauer A, Maurer CM, Schonthaler HB, Neuhauss SC. Phylogenetic analysis of the vertebrate excitatory/neutral amino acid transporter (SLC1/EAAT) family reveals lineage specific subfamilies. BMC evolutionary biology. 2010;10:117.
17. Rasko JE, Battini JL, Gottschalk RJ, Mazo I, Miller AD. The RD114/simian type D retrovirus receptor is a neutral amino acid transporter. Proceedings of the National Academy of Sciences of the United States of America. 1999;96(5):2129-34.
18. Sommerfelt MA, Weiss RA. Receptor interference groups of 20 retroviruses plating on human cells. Virology. 1990;176(1):58-69.
19. Tailor CS, Nouri A, Zhao Y, Takeuchi Y, Kabat D. A sodium-dependent neutral-amino-acid transporter mediates infections of feline and baboon endogenous retroviruses and simian type D retroviruses. Journal of virology. 1999;73(5):4470-4.
20. Funk M, Cornelis G, Vernochet C, Heidmann O, Dupressoir A, Conley A, et al. Capture of a Hyena-Specific Retroviral Envelope Gene with Placental Expression Associated in Evolution with the Unique Emergence among Carnivorans of Hemochorial Placentation in Hyaenidae. Journal of virology. 2019;93(4).
21. Heidmann O, Vernochet C, Dupressoir A, Heidmann T. Identification of an endogenous retroviral envelope gene with fusogenic activity and placenta-specific expression in the rabbit: a new "syncytin"

in a third order of mammals. Retrovirology. 2009;6:107.

22. Malicorne S, Vernochet C, Cornelis G, Mulot B, Delsuc F, Heidmann O, et al. Genome-Wide Screening of Retroviral Envelope Genes in the Nine-Banded Armadillo (Dasypus novemcinctus, Xenarthra) Reveals an Unfixed Chimeric Endogenous Betaretrovirus Using the ASCT2 Receptor. Journal of virology. 2016;90(18):8132-49.
23. Marin M, Lavillette D, Kelly SM, Kabat D. N-linked glycosylation and sequence changes in a critical negative control region of the ASCT1 and ASCT2 neutral amino acid transporters determine their retroviral receptor functions. Journal of virology. 2003;77(5):2936-45.
24. Garaeva AA, Guskov A, Slotboom DJ, Paulino C. A one-gate elevator mechanism for the human neutral amino acid transporter ASCT2. Nat Commun. 2019;10(1):3427.
25. Garaeva AA, Oostergetel GT, Gati C, Guskov A, Paulino C, Slotboom DJ. Cryo-EM structure of the human neutral amino acid transporter ASCT2. Nature structural & molecular biology. 2018;25(6):515-21.
26. Console L, Scalise M, Tarmakova Z, Coe IR, Indiveri C. N-linked glycosylation of human SLC1A5 (ASCT2) transporter is critical for trafficking to membrane. Biochimica et biophysica acta. 2015;1853(7):1636-45.
27. Capon DJ, Chamow SM, Mordenti J, Marsters SA, Gregory T, Mitsuya H, et al. Designing CD4 immunoadhesins for AIDS therapy. Nature. 1989;337(6207):525-31.
28. Holmen SL, Federspiel MJ. Selection of a subgroup A avian leukosis virus [ALV(A)] envelope resistant to soluble ALV(A) surface glycoprotein. Virology. 2000;273(2):364-73.
29. Zingler K, Young JA. Residue Trp-48 of Tva is critical for viral entry but not for high-affinity binding to the SU glycoprotein of subgroup A avian leukosis and sarcoma viruses. Journal of virology. 1996;70(11):7510-6.
30. Cornelis G, Heidmann O, Degrelle SA, Vernochet C, Lavialle C, Letzelter C, et al. Captured retroviral envelope syncytin gene associated with the unique placental structure of higher ruminants. Proceedings of the National Academy of Sciences of the United States of America. 2013;110(9):E828-37.
31. Redelsperger F, Cornelis G, Vernochet C, Tennant BC, Catzeflis F, Mulot B, et al. Capture of syncytin-Mar1, a fusogenic endogenous retroviral envelope gene involved in placentation in the Rodentia squirrel-related clade. Journal of virology. 2014;88(14):7915-28.
32. Buchrieser J, Degrelle SA, Couderc T, Nevers Q, Disson O, Manet C, et al. IFITM proteins inhibit placental syncytiotrophoblast formation and promote fetal demise. Science. 2019;365(6449):176-80.
33. Garcia-Murria MJ, Exposito-Dominguez N, Duart G, Mingarro I, Martinez-Gil L. A Bimolecular Multicellular Complementation System for the Detection of Syncytium Formation: A New Methodology for the Identification of Nipah Virus Entry Inhibitors. Viruses. 2019;11(3).
34. Yamamoto M, Matsuyama S, Li X, Takeda M, Kawaguchi Y, Inoue JI, et al. Identification of Nafamostat as a Potent Inhibitor of Middle East Respiratory Syndrome Coronavirus S Protein-

Mediated Membrane Fusion Using the Split-Protein-Based Cell-Cell Fusion Assay. Antimicrob Agents Chemother. 2016;60(11):6532-9.

35. Senigl F, Plachy J, Hejnar J. The core element of a CpG island protects avian sarcoma and leukosis virus-derived vectors from transcriptional silencing. Journal of virology. 2008;82(16):7818-27.
36. Pecenka V, Dvorak M, Travnicek M. Avian nephroblastomas induced by a retrovirus (MAV-2) lacking oncogene. I. Construction of MAV-1 and MAV-2 proviral restriction maps and preparation of specific proviral molecular subclones. Folia Biol (Praha). 1988;34(3):129-46.
37. Yan RT, Wang SZ. Production of high-titer RCAS retrovirus. Methods Mol Biol. 2012;884:193-9.
38. Petropoulos CJ, Hughes SH. Replication-competent retrovirus vectors for the transfer and expression of gene cassettes in avian cells. Journal of virology. 1991;65(7):3728-37.
39. Mallet F, Bouton O, Prudhomme S, Cheynet V, Oriol G, Bonnaud B, et al. The endogenous retroviral locus ERVWE1 is a bona fide gene involved in hominoid placental physiology. Proceedings of the National Academy of Sciences of the United States of America. 2004;101(6):1731-6.
40. Schaefer-Klein J, Givol I, Barsov EV, Whitcomb JM, VanBrocklin M, Foster DN, et al. The EV-O-derived cell line DF-1 supports the efficient replication of avian leukosis-sarcoma viruses and vectors. Virology. 1998;248(2):305-11.
41. Plachy J, Kotab J, Divina P, Reinisova M, Senigl F, Hejnar J. Proviruses selected for high and stable expression of transduced genes accumulate in broadly transcribed genome areas. Journal of virology. 2010;84(9):4204-11.
42. Rainey GJ, Natonson A, Maxfield LF, Coffin JM. Mechanisms of avian retroviral host range extension. Journal of virology. 2003;77(12):6709-19.

Figures

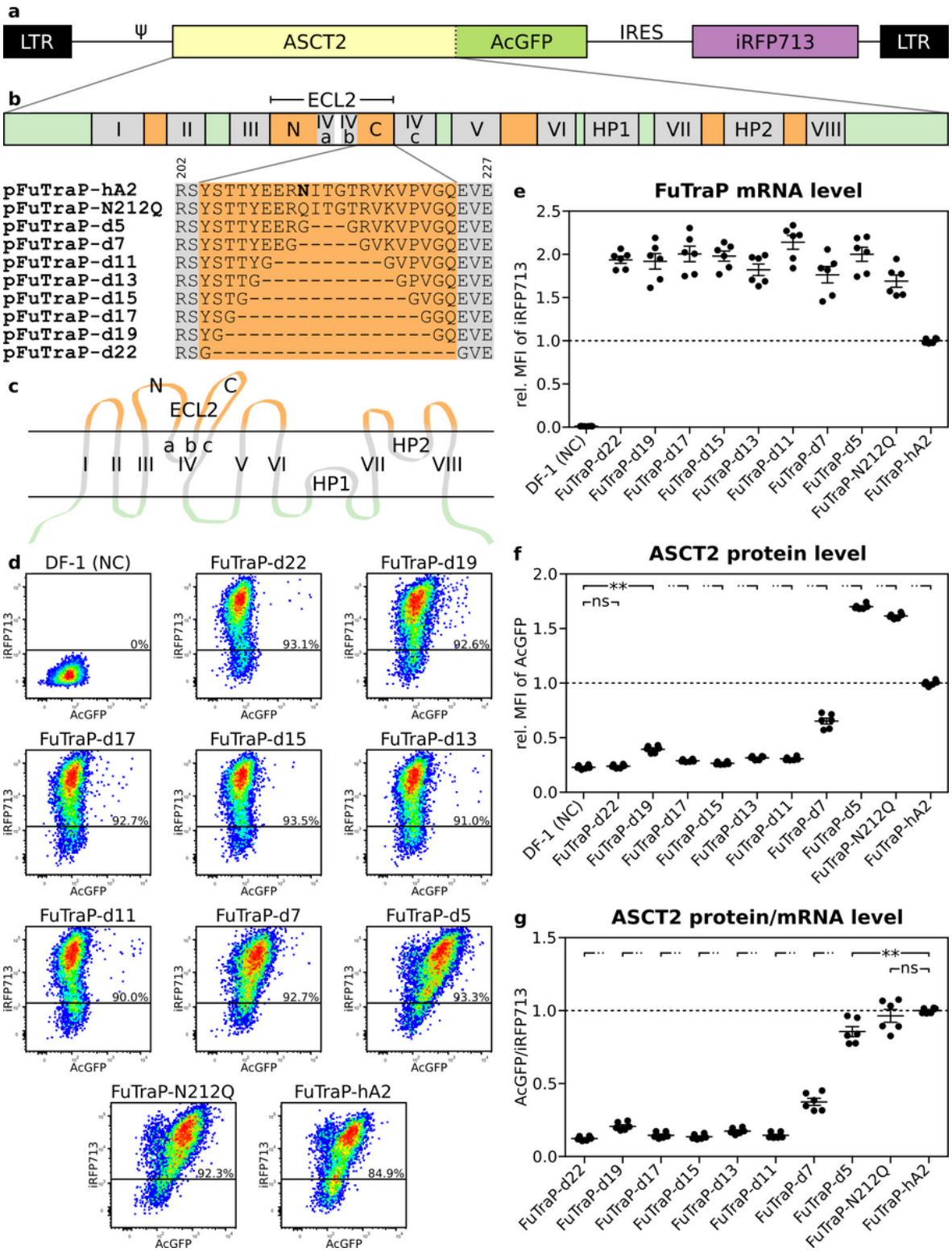

Figure 1

pFuTraP vectors and ASCT2 expression a. Scheme of the pFuTraP-hA2 vector. The vector was constructed using MAV LTRs, RCASBP encapsidation signal (Ψ), human ASCT2 fused with AcGFP, IRES, and iRFP713 fluorescent marker. b. Scheme of the ASCT2 structure and alignment of mutants. Depicted are eight transmembrane helices and two helical hairpins (displayed in grey, numbered I-VIII and HP1-2, respectively), which divide the protein into intracellular (light green) and extracellular parts (orange). The

longest extracellular loop (ECL2) is interrupted by short membrane regions (IVa and IVb) to the N-terminal (region N) and C-terminal (region C) parts. Region C is stabilised by two antiparallel beta-sheets and was proposed as a retroviral docking site. The amino acid sequences of ASCT2 mutants with deglycosylated and shortened region C used in this study are shown. The glycosylated asparagines are shown in bold. c. Scheme of membrane topology of ASCT2. d. iRFP713 and AcGFP expression from pFuTraP vectors. DF-1 cells with ectopic expression of pFuTraP vectors were characterised by flow cytometry. The analysis was repeated three times in biological duplicates and representative dot plots of 104 cells are presented. The X-axis depicts the AcGFP fluorescence, Y-axis depicts the iRFP713 fluorescence. iRFP713-positive cells are gated. e. iRFP713 fluorescence reflects the level of RNA produced from pFuTraP vectors. The MFI of iRFP713 of individual variants relative to the wild-type FuTraP-hA2 is plotted. f. AcGFP fluorescence reflects the level of ASCT2 protein produced from pFuTraP vectors. The MFI of AcGFP of individual variants relative to the wild-type FuTraP-hA2 is plotted. g. ASCT2 protein production from pFuTraP vectors. The relative MFI of ASCT2-AcGFP of individual variants was normalised to the relative MFI of iRFP713 (mRNA level). NC, negative control (non-modified DF-1 cells). Data is shown as means + standard errors, **$p<0.01$, Mann–Whitney two-tailed test.

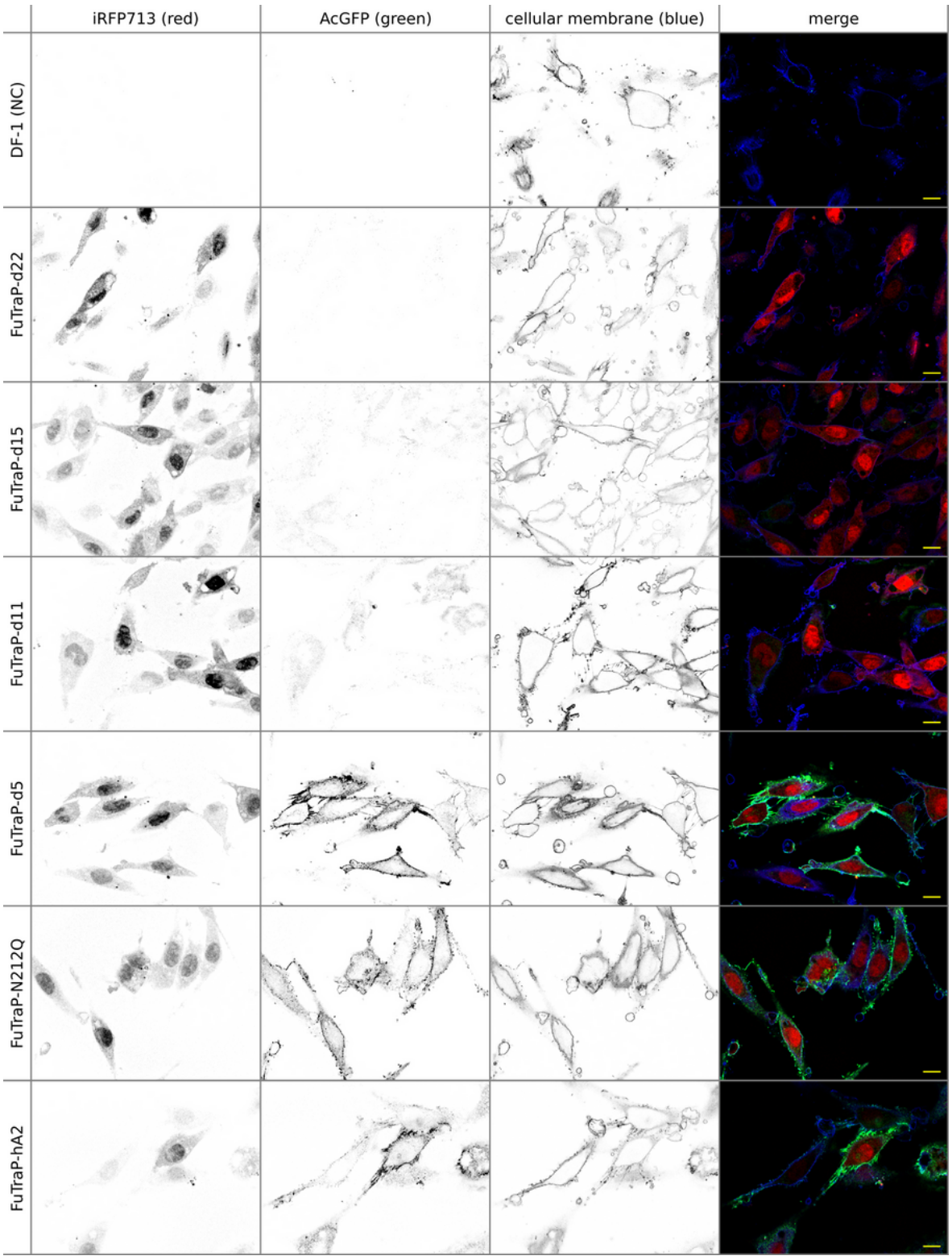

Figure 2

Localisation of selected ASCT2 variants expressed from the pFuTraP vector Confocal microscopy analysis of the IRES-driven iRFP713 (red channel, left), AcGFP fused with ASCT2 (green channel, middle left), and the stained cellular membrane (blue channel, middle right). The channels are depicted separately in grayscale and merged into the colourised composites (right). Non-modified DF-1 cells (NC)

and DF-1 cells modified with FuTraP-d22, FuTraP-d15, FuTraP-d11, FuTraP-d5, FuTraP-N212Q, and the wild-type FuTraP-hA2 (from top to the bottom) are shown. Scale bars represent 10 μm.

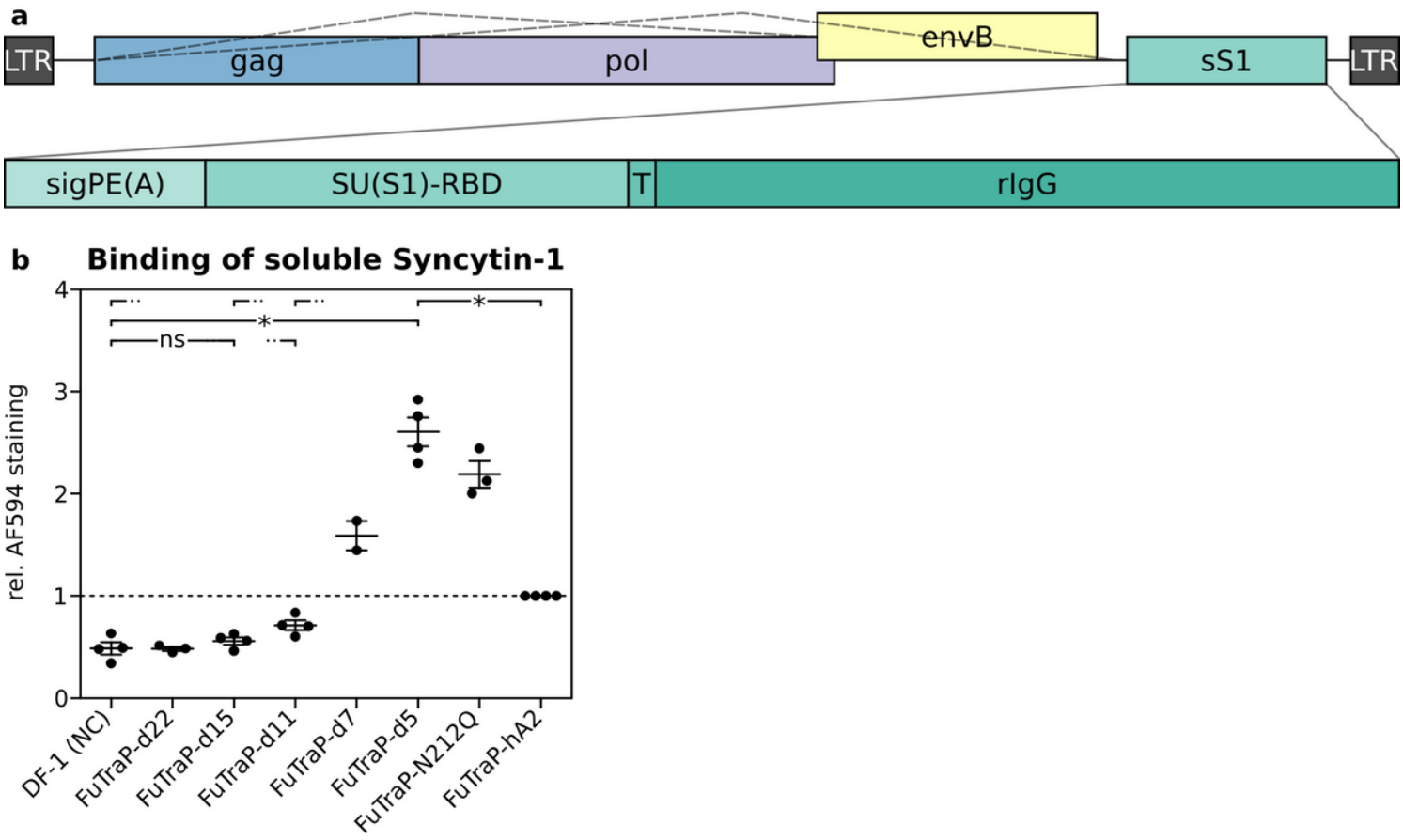

Figure 3

Binding of soluble Syncytin-1 to the selected ASCT2 variants a. Schematic representation of the vector expressing the soluble form of Syncytin-1 (sS1). The sS1 (turquoise) was cloned downstream of the splice acceptor (dashed line) of replication-competent avian retrovirus RCASBP(B), which permits propagation in cell culture and shedding of sS1 into the supernatant. sS1 consists of the signal peptide of Env(A) (sigPE(A)) followed in-frame by the receptor-binding domain of Syncytin-1 (SU(S1)-RBD), Tobacco Etch Virus protease cleavage site (T), and rabbit heavy chain of IgG (rIgG). The sS1 protein produced to the supernatant was used for the cell surface labelling of ASCT2 variants. b. Labelling of living cells with sS1. Cells expressing either modified or wild-type ASCT2 were incubated with sS1, and its binding to ASCT2 was visualised by staining with anti-rabbit IgG antibody conjugated to Alexa Fluor 594. Median of Alexa Fluor 594 fluorescence intensity was measured by flow cytometry for individual ASCT2 variants and normalised to the wild-type FuTraP-hA2 (Y axis). Non-modified DF-1 cells labelled with sS1 represent the negative control (NC). Results of two (FuTraP-d7), three (FuTraP-d22, FuTraP-N212Q) or four (the rest) independent experiments are shown. Data is shown as means + standard errors, *p<0.05, the lower number of measurements was not sufficient for statistical evaluation by the Mann-Whitney test.

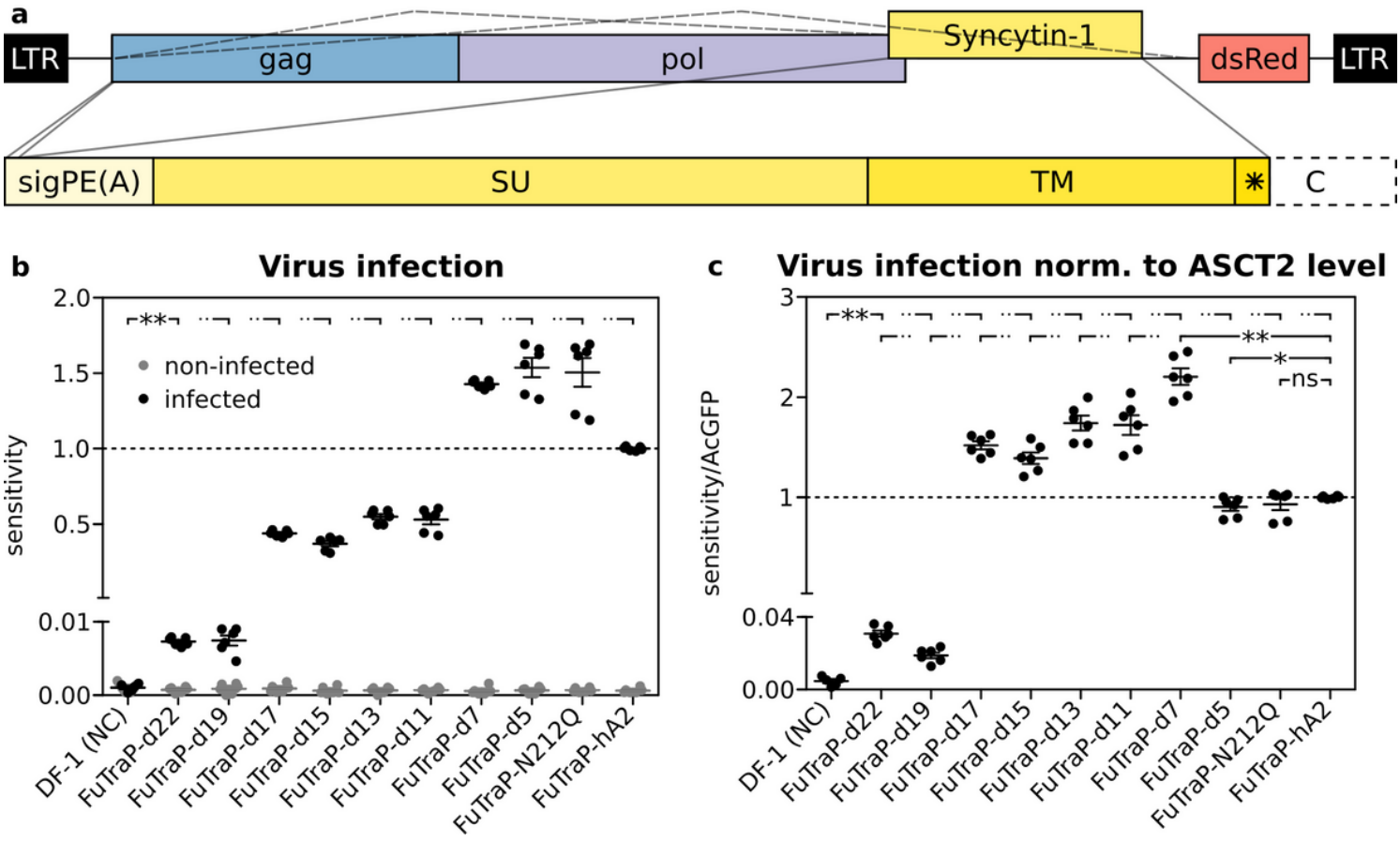

Figure 4

Syncytin-1 virus infection of cells expressing the FuTraP variants a. Scheme of the pMCAS(Sync1-MSC16)dsRed vector used for virus production. The envelope of the virus consisted of the signal peptide of Env(A) (sigPE(A)) followed in-frame by Syncytin-1 SU and TM. The mutated cryptic splice acceptor is depicted by an asterisk in the cytoplasmic tail (C), which was truncated to 16 amino acids. Dashed lines indicate alternative splicing generating Syncytin-1 mRNA and dsRed mRNA. b. Infection of cells expressing variants of FuTraP-ASCT2 with Syncytin-1-enveloped virus. Infected cells were identified by flow cytometry as dsRed positive. Results of three independent experiments in biological duplicates are plotted. See Additional File 1: Fig. S1 for representative dot plots. c. Normalised ASCT2 receptor sensitivity. The sensitivity of the FuTraP variant to the virus was further normalised to ASCT2-AcGFP MFI levels. This normalisation linked the receptor sensitivity quantitatively to its protein level. The data corresponds to sensitivity/AcGFP MFI of ASCT2 variants relative to sensitivity/AcGFP MFI of the wild-type FuTraP-hA2. NC, negative control (non-modified DF-1 cells). Data is shown as means + standard errors, *p<0.05, **p<0.01, Mann–Whitney two-tailed test.

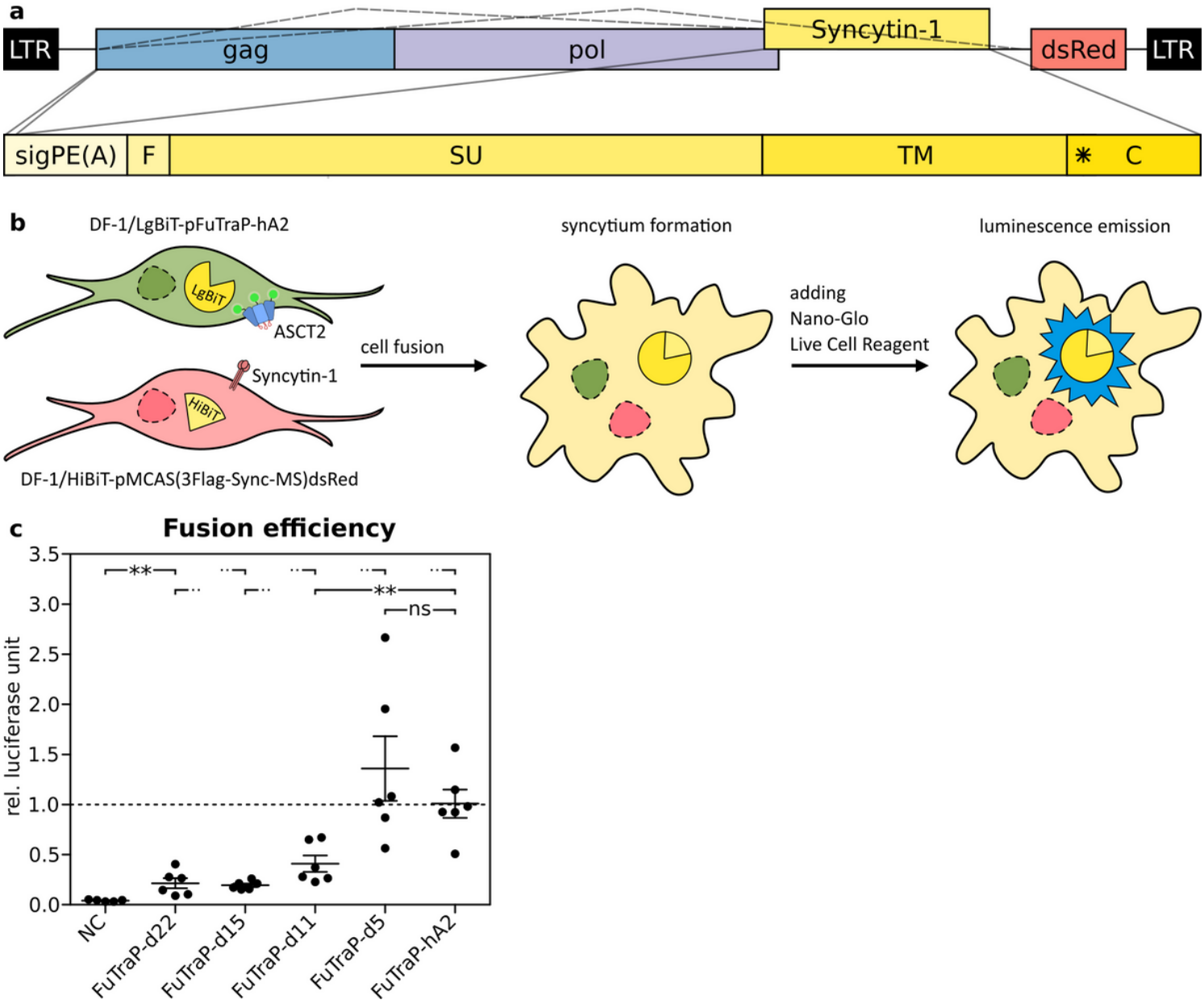

Figure 5

Cell-cell fusion luciferase assay a. Scheme of the pMCAS(3Flag-Sync1-MS)dsRed construct used for luciferase assay. The signal peptide of Env(A) (sigPE(A)) was followed in-frame by the three-Flag epitope (F), Syncytin-1 SU and TM subunits. The construct contained the full-length cytoplasmic tail of Syncytin-1 (C). The mutated cryptic splice acceptor is depicted by an asterisk, dashed lines indicate the alternative splicing generating Syncytin-1 and dsRed mRNAs. b. Scheme of the luciferase assay using NanoBiT technology. Two subunits of NanoLuc luciferase, LgBiT and HiBiT, were transfected into a DF-1 cell line separately and stable transfectants were selected. Cells expressing the LgBiT part of NanoLuc luciferase were transduced with FuTraP variants and sorted (green). Cells expressing HiBiT were transiently transfected by pMCAS(3Flag-Sync1-MS)dsRed (red). A mixture of LgBiT and HiBiT expressing cells was seeded. The interaction of human ASCT2 with Syncytin-1 triggered cell-cell fusion followed by complementation of LgBiT by HiBiT. After substrate addition, the luminescence emission signal was

quantified. c. Efficiency of cell-cell fusion induced by the interaction of Syncytin-1 with the wild-type or mutant ASCT2 receptor measured by luciferase assay. Data corresponds to luciferase units detected for the selected FuTraP variants relative to luciferase units detected for the wild-type FuTraP-hA2. DF-1/LgBiT cells without ASCT2 mixed with DF-1/HiBiT-Syncytin-1 cells were used as a negative control (NC). Experiment was performed twice in biological triplicates. Data is shown as means + standard errors, **p<0.01, Mann–Whitney two-tailed test.

Supplementary Files

This is a list of supplementary files associated with this preprint. Click to download.

- FigS1.png
- FigS2.png
- FigS3.png
- Movie.mp4
- pFuTraPN212Q.gb
- pFuTraPd11.gb
- pFuTraPd13.gb
- pFuTraPd15.gb
- pFuTraPd17.gb
- pFuTraPd19.gb
- pFuTraPd22.gb
- pFuTraPd5.gb
- pFuTraPd7.gb
- pFuTraPhA2.gb
- pMCAS3FLAGSync1MSdsRed.gb
- pMCASsync1MSC16dsRed.gb
- pSUS1RBDIgG.gb